Federico Di Traglia · Stefania Bartolini · Erica Artesi · Teresa Nolesini · Andrea Ciampalini · Daniela Lagomarsino · Joan Martí · Nicola Casagli

Susceptibility of intrusion-related landslides at volcanic islands: the Stromboli case study

Abstract Susceptibility of intrusion-related landslides in an active volcano was evaluated coupling the landslide susceptibility estimation by random forest (RF), and the probabilistic volcanic vent opening distribution, as proxy for magma injection, using the QVAST tool. In order to develop and test the method proposed here, the RF/QVAST approach was adopted for Stromboli volcano (Southern Italy) since it experienced moderate to huge instability events, it is geomorphologically prone to instability events, and it is affected by active intense volcanic activity that can produce slope instability. The main destabilizing factors of the volcanic flanks are the slope, the aspect, the terrain roughness, the land cover and the litho-technical features of the outcropping rocks. Estimation of volcanic susceptibility shows that the areas with high probability of new vent opening are located in the north-western unstable volcano flank (Sciara del Fuoco), in the volcano summit and the north-eastern volcano flank coherent with the possible re-activation of the eruptive fissures related to the regional tectonic setting. The areas with higher probability of intrusion-related landslides are located in the upper part of the Sciara del Fuoco, while the rest of the island show moderate to low probability of intrusion-related landslide occurrence.

Keywords Volcano slope instability · Landslides susceptibility · Volcanic susceptibility · Stromboli · Aeolian Islands

Introduction

Volcano instability is defined as the condition for a volcanic edifice to be destabilized to a degree sufficient to increase the likelihood of the structural failure of all or part of the edifice (Voight and Elsworth 1997). Landslides in volcanic terrains comprise a wide spectrum of phenomena, from shallow debris remobilization (small rock falls, dry or wet debris flows) to large-scale slope deformation, eventually evolving into large lateral collapse of the volcanic edifice with the emplacement of rockslide-debris avalanches of tens to hundreds of km³ (Siebert 1984; Sosio et al. 2012). These events may potentially cause severe damage to human society, directly or through secondary events like tsunamis and lahars (Siebert 1984; Major et al. 2000; Bonaccorso et al. 2003). Smaller landslides at active volcanoes are often associated with the precursory activity of larger collapses (Voight et al. 2002). Even when they are not the main hazard issue, mass-wasting may cause long-lasting hazard factor in volcanic setting, due to the persistency of non-equilibrium slope conditions (Major et al. 2000).

Slope failure may occur in response to active deformation (magma intrusion, gas overpressure, substrate spreading) or may result over a long period due to over-steepening, over-loading, or peripheral erosion (Voight and Elsworth 1997). Slope stability is diminished by magmastatic and magma overpressures that accompany intrusion in unstable flanks (Tibaldi et al. 2009). Excess pore pressures in potential failure zones can be generated as a result of intrusion-related mechanical or thermal straining of the rock-fluid medium, pressurized retrograde boiling in high level magma chambers, or hydrothermal fluid circulation (Voight and Elsworth 1997), reducing the resistance to sliding. In addition, tectonic activity can generate earthquakes that may aid slope instability through inertial forces and shaking-induced pore pressure generation (Hazlett et al. 1991).

In this study, landslide susceptibility (LS) was estimated considering the combination of morphological features (e.g., slope angle, slope direction, etc) and geomechanical rock properties characterizing the Island of Stromboli (Fig. 1). Moreover, volcanic susceptibility (VS, i.e., the probability of new vent opening) was estimated. The combination of LS and VS was used as proxy of intrusion-related landslide susceptibility. The effects of other triggers (rainfall, sea waves, seismic shaking) were not considered here. The landslides predisposing factors were estimated by random forest (RF) technique (Catani et al. 2013; Ciampalini et al. 2015), while the probabilistic volcanic vent opening distribution, as proxy for magma injection, was evaluated by QVAST tool (Bartolini et al. 2013). The reasons to apply this methodology to Stromboli volcano are based on the following facts: (i) it has experienced moderate to huge landslides (Tibaldi 2001), (ii) it is geomorphologically prone to instability events (Nolesini et al. 2013), (iii) it is affected by active intense volcanic activity that can significantly affect the stability of slopes (Di Traglia et al. 2014a) and (iv) its flank instability could affect areas inhabited and intensely frequented by people for touristic activities (Nave et al. 2010). This work is based on a large amount of existing information, mainly derived from scientific papers, and from elaboration of topographic data, both collected in a dedicated geo-database. This paper is focussed on testing the impact of the application of the proposed method on the final result, rather than on the comparison of existing methodologies.

Geological setting

Stromboli Volcano, located in the Tyrrhenian Sea off the southern coast of Italy (Fig. 1), is the north-eastern most tip of the Aeolian volcanic arc, comprising islands and seamounts of volcanic origin. The Aeolian Islands are characterized by a typical semi-arid Mediterranean condition, with a mean annual precipitation of 602 mm, mostly falling in autumn and winter (Kokelaar and Romagnoli 1995).

Stromboli was affected by several mass-wasting events during its geological history, mainly located in the NW part of the volcano that produced a depression called "Sciara del Fuoco" (SdF). Stromboli is characterized by intermittent mild explosions occurring at a typical rate of 1–10 events per hour (Strombolian activity; Blackburn et al. 1976). The ordinary Strombolian activity is occasionally interrupted by the occurrence of higher-intensity explosions, usually referred to as "major" or "paroxysmal" events, based on the explosion intensity (Rosi et al. 2013). The explosive
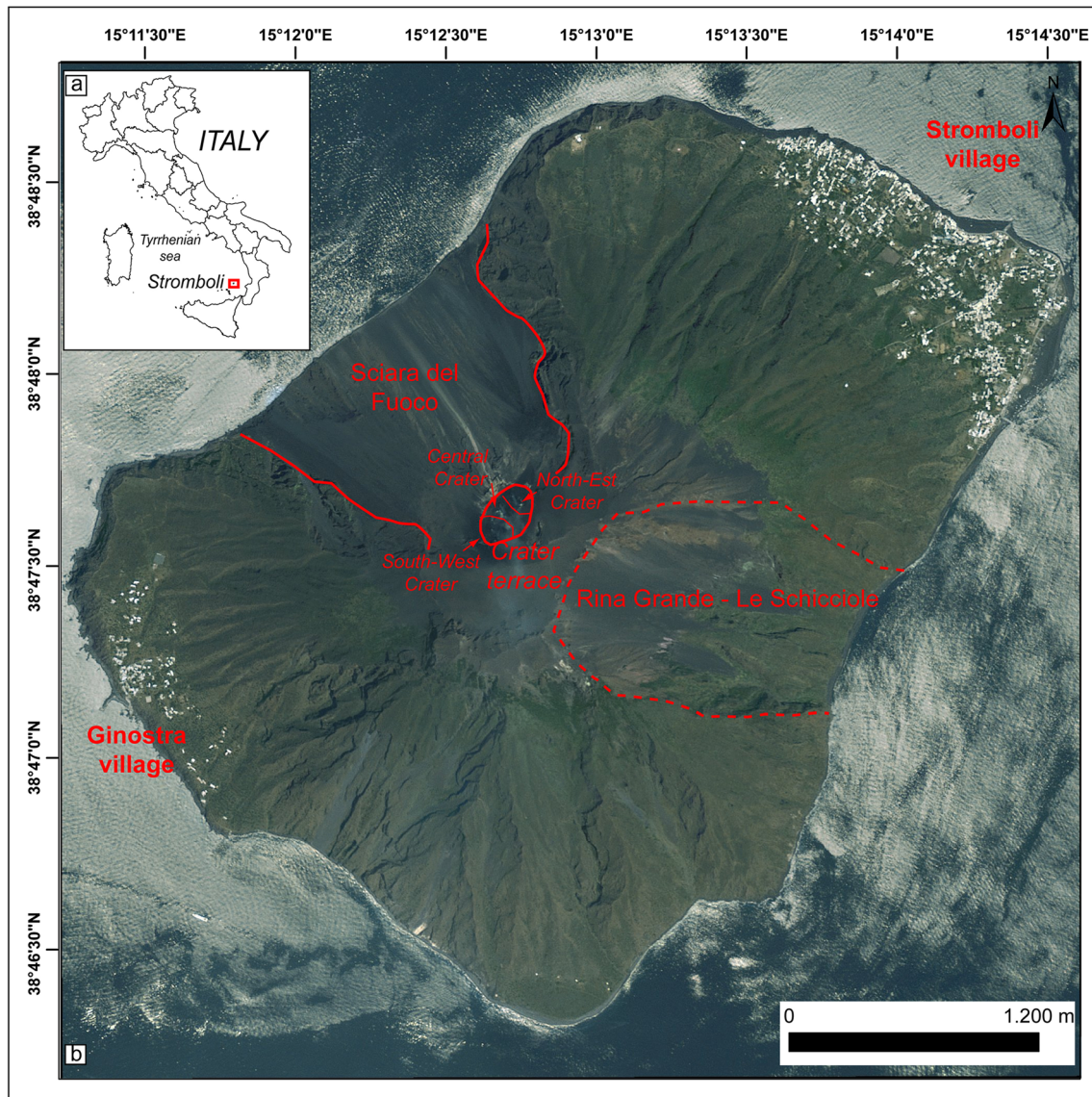
Fig. 1 a Geographic setting of the Island of Stromboli. **b** SPOT satellite image (2009) of the Island of Stromboli, highlighting the two settlements (Stromboli and Ginostra villages) and the main active volcanological features (the crater terrace and the Sciara del Fuoco)

activity is confined in the crater terrace, comprising the NE Crater zone (NEC), Central Crater zone (CC) and SW Crater zone (SWC), located at ~750 m above sea level (a.s.l.) at the headwall of the SdF (Calvari et al. 2014). Ephemeral vents fed flank eruptions (1 every 5 years; Rosi et al. 2013), which opened at different heights but almost always confined in the SdF (Tibaldi et al. 2009), and were often associated with tsunamis (1 every 20 years; Rosi et al. 2013). The last flank eruption occurred inside the SdF and lasted 4 months from August to November 2014 (Di Traglia et al. 2015; Rizzo et al. 2015; Zakšek et al. 2015), whereas outside the SdF, the last episode dates back to the Roman age (Arrighi et al. 2004). The SdF depression is filled with volcaniclastic deposits and lavas (Apuani et al. 2005a), emitted from the strombolian activity and lava flows from the summit crater terrace and the ephemeral vents within the SdF (Rosi et al. 2013).

Slope instability phenomena at Stromboli (Table 1; Fig. 2) are common and frequently associated with the effusive

phases. At the onset of the 1985, 2002–2003, 2007 and 2014 flank eruptions, *gravel/debris slides* evolved in *dry gravel/debris flows* along the SdF following the opening of eruptive fissures on the NE flank of the summit cone (De Fino et al. 1988; Calvari et al. 2005, 2010; Carlà et al. 2016). During the 2012–2013 high-intensity strombolian activity, overflows occurred and were often associated with the sliding of the NEC crater-rim (Di Traglia et al. 2014b; Calvari et al. 2016). During the 2002–2003 flank eruption, a rock rotational slide (25–30 × 10⁶ m³) occurred (Bonaccorso et al. 2003). This phenomenon was triggered by the injection of a lateral intrusion (Neri et al. 2008) and caused two tsunamis, which affected the coastline with a maximum run-up of 6–7 m at Stromboli village (Tinti et al. 2005). The submarine flanks of Stromboli volcano are characterized by mass-wasting, affecting a large part of the entire submarine area and often influencing the stability of subaerial slopes (Casalbore et al. 2010).

Table 1 Classification of slope instability phenomena at Stromboli volcano

Classification	Description	Volume
"Deep-seated gravitational slope deformations" evolving in *"rock avalanches"*	Large-scale gravitational deformation of the Sciara del Fuoco, manifested by scarps, benches, cracks, trenches and bulges, but lacking a fully defined rupture surface evolving in extremely rapid, massive, flow-like motion of fragmented rock	$>10^7$ m^3
"Rock (rotational or planar) slide" evolving in *"rock avalanches"*	Sliding of a mass of weak rock on rotational rupture surface which is not structurally controlled or sliding of a mass of rock on a planar rupture surface evolving in extremely rapid, massive, flow-like motion of fragmented rock	10^6–10^7 m^3
"Rock fall" evolving in dry *"gravel/debris flows"*	Detachment, fall, rolling and bouncing of rock evolving in (generally) rapid flow-like movement of loose dry, sorted or unsorted granular material, without excess pore pressure	$<10^6$ m^3 (typically $\approx 10^4$ m^3)
"Gravel/debris slide" evolving in dry *"gravel/debris flows"*	Sliding of a mass of granular material on a shallow, planar surface parallel with the ground evolving in (generally) rapid flow-like movement of loose dry, sorted or unsorted granular material, without excess pore pressure. Detachment areas are mainly located in the Sciara del Fuoco and in the slopes around the crater terrace	$<10^6$ m^3 (typically $\approx 10^5$ m^3)

Methods

Geo-database generation

The geo-database of the Stromboli Island was developed in three different phases: (i) ancillary data collection, (ii) database design and (iii) product generation (Ciampalini et al. 2015). All the ancillary data were included in a dedicated database (Fig. 3) comprising different thematic maps (geological, land cover and landslide inventory maps, digital elevation models (DEM), very high-resolution (VHR) optical photos). Morphometric data of the island was produced using DEMs with a 10 × 10-m resolution generated by the Istituto Nazionale di Geofisica e Vulcanologia (Tarquini et al. 2007, 2012). Landslide inventory map (LIM; Fig. 4) was constructed using VHR (0.5 × 0.5 m) DEM (Salvatici et al. 2016), and two Quickbird VHR-optical images were also used. The geology of the study area was retrieved using the geological maps of the Island of Stromboli (scale 1:10,000; Tibaldi 2010) in digital format. The geological information was classified in order to produce a litho-technical map. Stratovolcano is composed of rock layers with inequality distributed elastic properties (primarily Young's modulus), and volcanic slope instability depends partly on how fracture resistant the edifices are (Apuani et al. 2005a,b; Schaefer et al. 2015). In this work, the following classification for the Stromboli rocks was used (Apuani et al. 2005a,b):

1. Lava unit (L). Alternation of lava layers (more than 65%) and autoclastic breccia layers;
2. Lava–Breccia unit (LB). Alternation of lava layers (ranging from 35 to 65%) and breccia layers;
3. Breccia unit (B). Alternation of lava layers (less than 35%) and autoclastic breccia layers;
4. Pyroclastic deposits (P). Prevailing pyroclastic poorly welded breccias alternating with tuff and lapillistones.

The land cover was deduced by the updated (2000) Corine Land Cover map (scale 1:100,000). Each polygon was classified following the three levels of the Corine Land Cover classification (http://www.eea.europa.eu/publications/COR0-landcover). Moreover, the geo-database includes the following (Fig. 3):

- the location of past recognizable eruptive vents and fissures, derived from eruption accounts, reports, and scientific papers (Rittmann 1931; Abruzzese 1935, 1937, 1940; Gasparini et al. 1968; Capaldi et al. 1978; Corazzato et al. 2008; Neri and Lanzafame 2009; Calvari et al. 2011; Marsella et al. 2012; Di Traglia et al. 2015);
- the structural elements related to this volcanism such as faults identified by previous geological studies (Tibaldi 2001; Tibaldi et al. 2009), monitoring data (Bonaccorso 1998; Falsaperla et al. 1999) and geophysical and geochemical surveys (Finizola et al. 2002, 2003; Linde et al. 2014).

Landslide susceptibility

A random forest implementation based on Matlab (Matworks, version 7.11, treebagger object (RFtb) and methods) was used as a basic model for Landslides Susceptibility Maps (LSM; Catani et al. 2013). RF classification is a machine-learning algorithm for non-parametric multivariate classification (Breiman 2001). The algorithm exploits random binary trees, which use a subset of the observations through bootstrapping techniques (Catani et al. 2013). In particular, from the original data set, a random selection of the training data is sampled and used to build the model; the data not included are referred to as "out-of-bag" (OOB; Breiman 2001). Moreover, a random selection of predictor variables is used to split each node of the trees (LSM; Catani et al. 2013). Each tree is developed to minimize classification errors, but the random selection influences the results, thus making a single-tree classification very unstable (Catani et al. 2013). For this reason, the RF-type methods make use of an ensemble of trees (the so-called "forest") thereby ensuring model stability (Catani et al. 2013). The choice of the input parameters, i.e. how many (and which) attributes should constitute the optimal configuration of the susceptibility assessment (conditioning variable, LCV), is a fundamental step in the susceptibility assessment process (Catani et al. 2013). The use of the RF treebagger algorithm provides quantitative estimates of variable importance, and therefore an initial and expert-driven selection of the input parameters is not necessary (Catani et al.
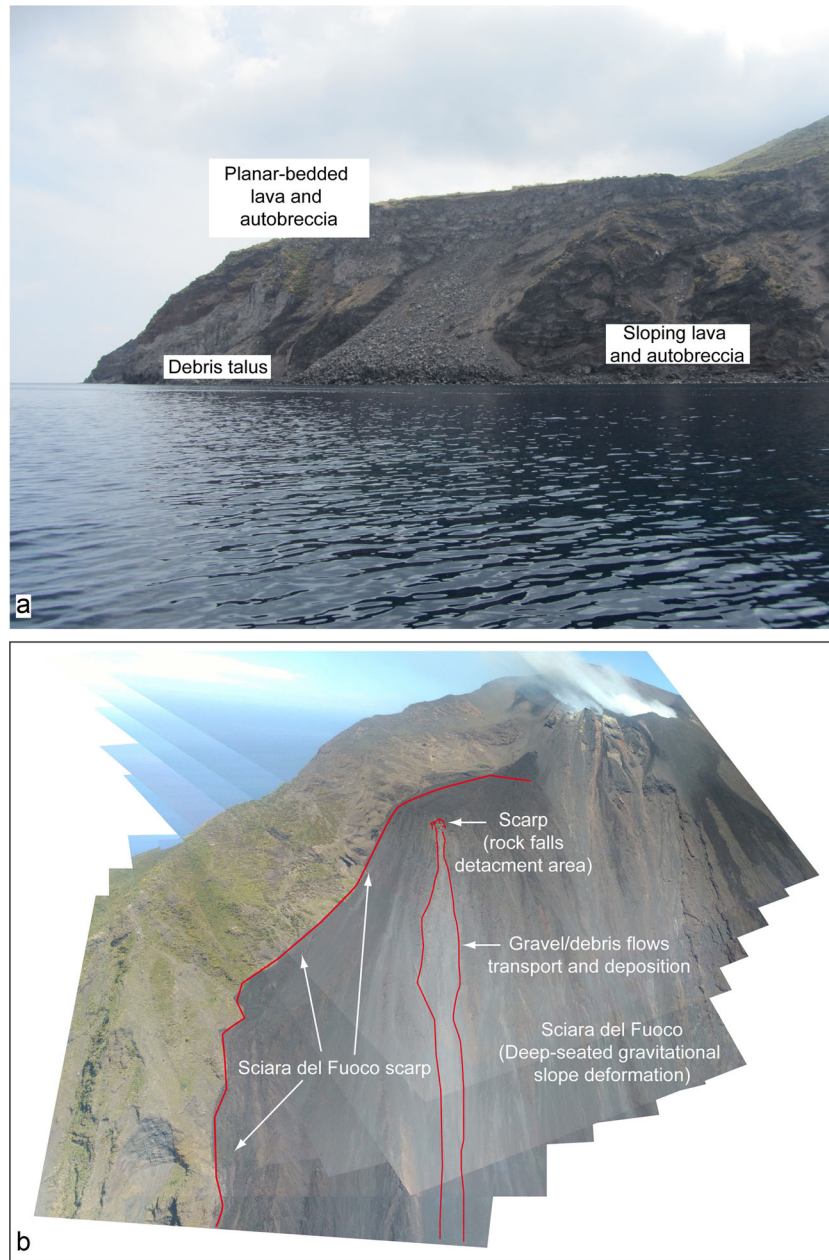
Fig. 2 Examples of mass-wasting at the island of Stromboli. **a** Rock falls affecting the coastal cliffs, mainly in the western part of the island as consequence of sea erosion acting on the lava units emplaced during the Neo-Stromboli period (26–13 ka). In **b**, the same area as observed from PLEIADES-1A panchromatic image (may 2016). **c** Rock fall evolving in dry gravel/debris flows within the Sciara del Fuoco depression, classified as deep-seated gravitation slope deformation

2013). For this reason, we prepared and performed tests where a fixed structure RFtb model is repeatedly run with decreasing total number of variables (LCV#). This means running the RFtb estimator with the complete LCV set and then removing one parameter at a time (the least important in terms of increase in prediction error when the variable is permuted across the out-of-bag observations, according to the Matlab function OOBPermutedVarDeltaError – http://www.mathworks.it/it/help/stats/treebagger.oobpermutedvardeltaerror.html), so as to reduce the parameter space. Every predictor set was applied to the test points and evaluated, in terms of misclassification probability (MP), to identify the optimal configuration for each working

resolution. This assessment is very important, especially when there is a limited possibility of increasing the training set along with the LCV#.

The DEM morphometric parameters, quantitatively used to characterize landforms and genetically related to geomorphologic processes and landslide susceptibility (Catani et al. 2013), were derived from calculation in Geographical Information System (GIS) environment. Several parameters were considered (using the focal operators and raster calculator of ESRI's ArcGIS 10.3), in order to avoid the subjectivity in the choice of explanatory variables: elevation, the terrain roughness (measured as the standard deviation of elevation, calculated on a 3 by 3 pixel kernel
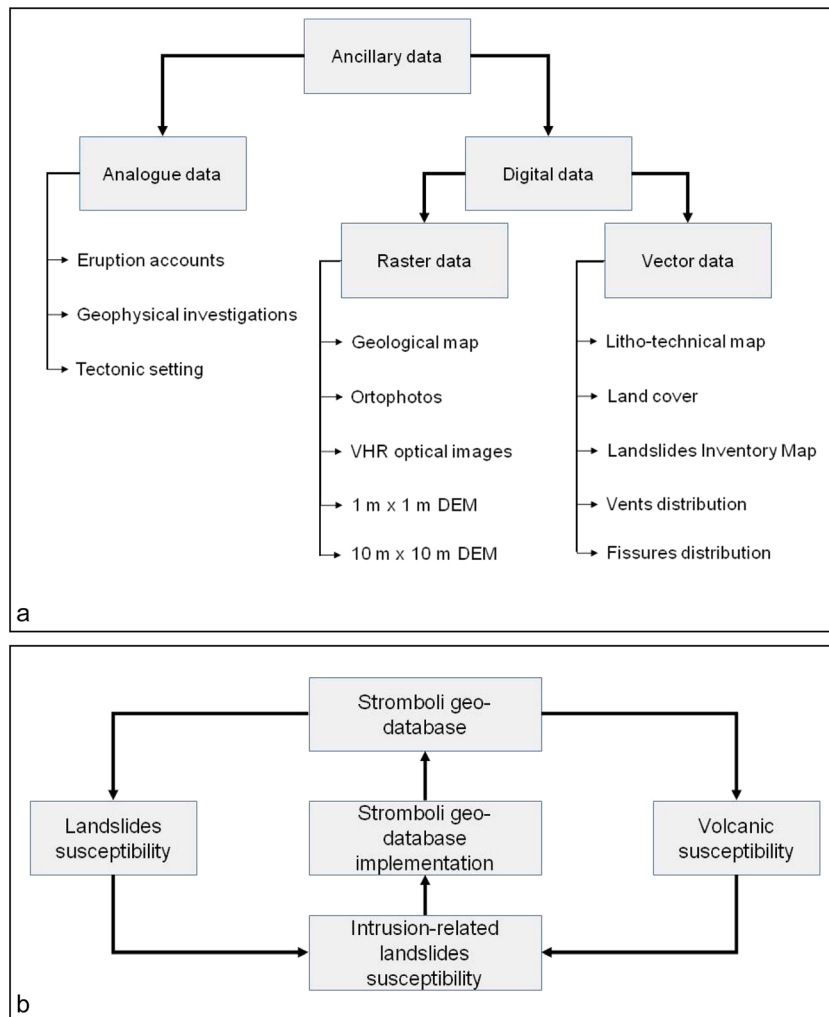
Fig. 3 **a** Workflow adopted in this study. All available data are collected in a dedicated geo-database. Selected thematic maps were extrapolated from the geo-database and used for landslides and volcanic susceptibility estimation. The final intrusion-related landslide susceptibility map, derived from the previously generated landslides and volcanic susceptibility maps, was re-integrated in the geo-database. **b** Workflow adopted in this study for the generation of the Stromboli geo-database. All digital data were collected in the Projected coordinate system: WGS 1984 UTM zone 33 Projection: Transverse Mercatore

window), curvature (general, planar, profile), slope, slope direction (aspect operator in ESRI's ArcGIS 10.3) and flow accumulation. Moreover, the land use and litho-technical features of the outcropping rocks were also considered. The complete description of the methodology applied to LSM generation is reported in Catani et al. (2013).

Volcanic susceptibility

The volcanic susceptibility is a spatial forecasting that allows calculating the probability of opening of new emission vents (Felpeto et al. 2007; Martí and Felpeto 2010). It is based on available volcano-structural data (fractures, faults, location of vents, eruptive fissures, etc.), which help to identify previous behaviour of the volcanic area, and on the changes occurring in regional and/or local stress fields originating from tectonic or lithological contrasts. One available tool to determine the volcanic susceptibility is QVAST tool (Bartolini et al. 2013), which determines the probability density function (PDF) based on kernel density estimation. This probabilistic method depends on the combination of different factors such as the size of the volcanic field, the degree of clustering and

the density of the volcano-structural data (Cappello et al. 2012; Bartolini et al. 2013; Becerril et al. 2013). For that reason, it requires the selection of an appropriate method for evaluating the bandwidth for the kernel function that allows calculating the volcanic susceptibility of the area, i.e. the probability of new vent opening, using direct and indirect structural data. The advantage to use QVAST lies in the possibility to choose between several approaches to determine the bandwidth for the kernel function, being this parameter the most important factor in representing the degree of randomness in the distribution of past events and determines the shape of the Gaussian kernel and, consequently, the resulting PDF.

In the case of Stromboli, the input parameters used for the spatial analysis were as follows (Fig. 4): (i) the location of past recognizable eruptive vents and (ii) the structural elements (fault, fissures, sheet intrusions) related to this volcanism, both collected in the geo-database.

The PDFs were obtained for each type of structural data with the method of the least square cross validation method (LSCV; Bartolini et al. 2013; Becerril et al. 2013) to obtain the bandwidth parameter, as it was the best method to represent the distribution of analysed data, and
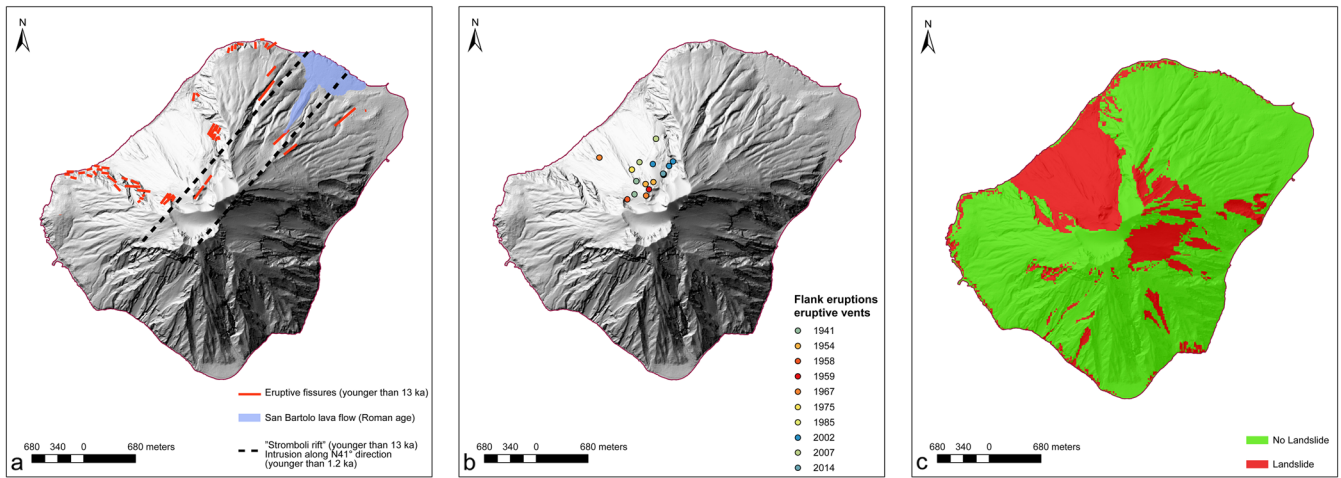
Fig. 4 a Structural data of the Island of Stromboli. Sub-areal eruptive fissures and outcropping sheet intrusions younger 13 ka. The distribution of the last eruptive event occurred outside the SdF depression (San Bartolo lava flow) is also reported. **b** Subaerial (*red dots*) and submarine (*orange dots*) vents (craters of isolated cinder cones, craters belonging to coalescent cinder cones and single craters). **c** Binary raster containing the distribution of landslides over the Island of Stromboli, derived from the Landslide Inventory Map (vector data)

were combined in a non-homogeneous Poisson process to obtain the final susceptibility map. The weights assigned were 0.6 for the vents, 0.3 for the faults and 0.1 for the fissures, which provided initial indicative probability distributions associated with each PDF. In particular, we have considered assigning these weights that the high probability of new vent opening is localized in the SdF depression. On the other hand, less probability has been assigned for the Holocene activity in the rift zone, along the NE-SW structural trend (Tibaldi et al. 2009), where only the San Bartolo lava flow occurred during the Roman age (Arrighi et al. 2004). The final susceptibility map represents those areas with greater or lesser probability of hosting a new vent.

Data presentation and discussion

The estimation of the landslides, volcanic and intrusion-related landslide susceptibility was developed in three different phases (Fig. 3): (i) generation of a dedicated geo-database, (ii) estimation of landslide susceptibility using the RF technique (Catani et al. 2013) and (iii) estimation of the probabilistic volcanic vent opening distribution, as proxy

for magma injection, based on available volcano-structural data (fractures, faults, location of vents, eruptive fissures, etc.; Fig. 4a, b), using the QVAST tool (Bartolini et al. 2013).

In the Landslides Inventory Map (Fig. 4c), 179 areas affected by mass-wasting phenomena were identified. Landslide dry gravel/debris slides evolving in dry gravel/debris flows are mainly located within the SdF and "Rina Grande-Le Schicciole" depressions, while they are scattered throughout the island and are for the most part related to the presence of Lava-Lava Breccia units. On the opposite, the sea-cliffs constituted by Lava unit are affected by rock-falls, related to strong coastal regression, mainly in the north-western side of the island.

The Landslides Susceptibility Map (LSM) of the Island of Stromboli (Fig. 5a) shows that the areas affected by high to very high landslide susceptibility include the Sciara del Fuoco, the upper part of the volcanic edifice and the coastal cliffs.

The performance of the model used was evaluated by building a receiver operating characteristic (ROC) curve (Fig. 6a). The performance of the model in terms of area under curve (AUC) was analysed
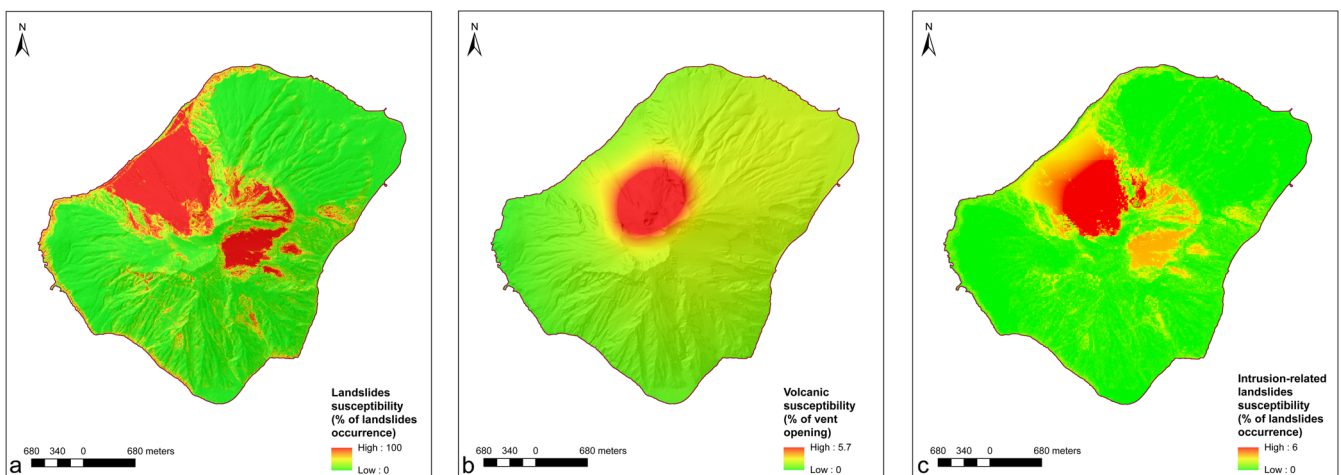

Fig. 5 a Landslide Susceptibility Map. **b** Volcanic Susceptibility Map, showing the spatial probability distribution of future volcanic eruptions. **c** Intrusion-related landslide susceptibility map of the Island of Stromboli. The background topographic data are the same of Fig. 4
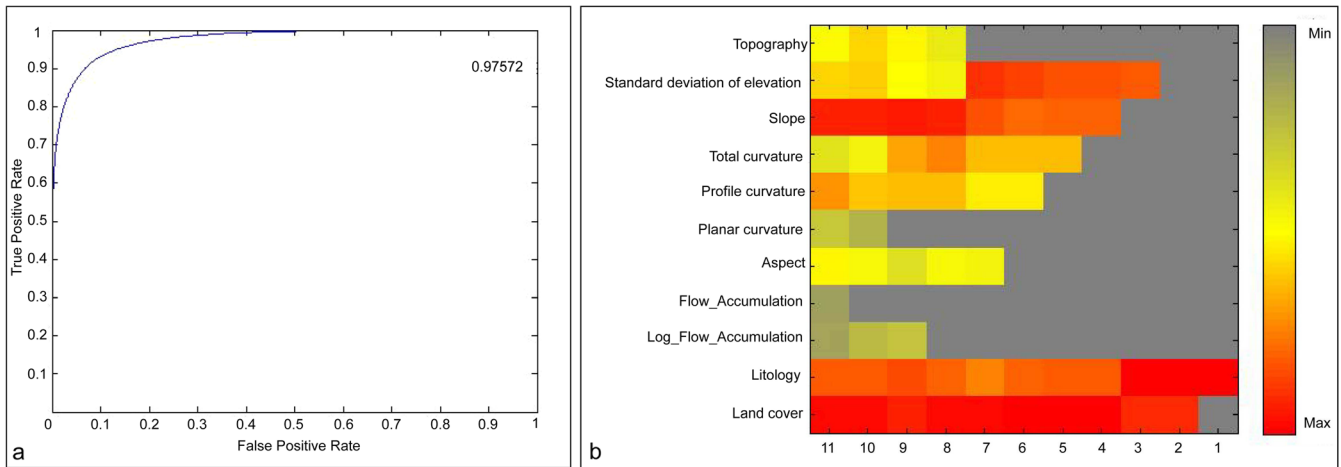
Fig. 6 **a** ROC plot and AUC value for the best classifications obtained at Stromboli. **b** Rank–LCV# plot illustrating the variation of parameter relative importance (expressed as rank using the colour ramp on the *right*) with parameter space (no. of parameters used LCV#) at the island of Stromboli. *Grey colours* correspond to combinations of LCV# in which the parameter importance was estimated as poor or where the parameter was discarded

using a constant minimum number of samples (mS#) proportion (10% of study area). The AUC values of 0.98 highlight very good results. This good finding can be due both to the scale of the analysis (10 m) and to the fact that the existence of the Sciara del Fuoco and Rina Grande–Le Schicciole zones greatly influences the localization of areas with high landslide susceptibility. The landslide conditioning variables (LCVs) ranking and significance (Fig. 6b) permit to better identify the landslide destabilizing factors. Considering the morphometric attributes, only the slope, the slope direction (aspect) and the terrain roughness (measured using the standard deviation of the elevation in a kernel 3 × 3) seem to have influence on landslide susceptibility, while the thematic attributes (land cover and the litho-technical) clearly control the landslide attitude. In particular, the slope, the terrain roughness and land cover are classified at higher rank, meaning that the parameters describing the potential for erosion and mass-wasting always influence the landslide susceptibility. The slope facing direction is a moderate-ranked LCV, while the landslide-prone areas are well identified based on the litho-technical features of the outcropping rocks. Most of the areas scarcely affected by mass-wasting phenomena are located at low- to moderate elevation (below 400 m a.s.l.), mainly in correspondence with lava units.

Probability of vent opening

In Fig. 5b, the final susceptibility map obtained using QVAST tool is shown. The result highlights the presence of a probability of new vent opening in the NE zone of Stromboli, where the presence of previous activity in the Holocene ensures the possibility of future eruptive vents. It is also shown that the area with the highest probability of vent opening is the area closest to the eruptive vent of the SdF depression, due to the current stress field in the island (Tibaldi et al. 2009).

Volcanic susceptibility map shows a probabilistic vent opening distribution elongated towards NE. This derives from the weights assigned for faults (0.3) and fissures (0.1) in the NE part of the island. The propagation of magma-filled crack (dykes) pattern is controlled by the current regional tectonic stress field and by the pre-existing structure (Anderson 1937; Takada 1994; Rubin 1995; Le Corvec et al. 2013). Since 13 ka, no sheets intruded the SW volcano flank, whereas summit eruptions took place

accompanied by a series of fissure eruptions along the opposite NE flank and sheeting around the SdF and within it (Tibaldi et al. 2009). The NE–SW rift system at Stromboli acted during historic times, as suggested by the eruption of the San Bartolo lava flow occurred during the Roman age (Arrighi et al. 2004). At Stromboli, the presence of debuttressing stresses due to the SdF forces the intrusion from the centre of the volcano to be injected towards the depression (Tibaldi et al. 2009). At the same time, the re-activation of the rift trend due to changing in regional stress could account for a new intrusion in the NE part of the island.

The integration of landslides and volcanic susceptibility maps allowed to generate the first "intrusion-related landslides susceptibility map" (Fig. 5c). The areas with higher probability of intrusion-related landslides are located in the upper part of the SdF, the same area characterized by the occurrence of mass-wasting during the 1985, 2002–2003, 2007 and 2014 flank eruptions (De Fino et al. 1988; Calvari et al. 2005, 2010; Carlà et al. 2016). The other area showing moderate susceptibility to intrusion-related landslides is the Rina Grande–Le Schicciole depression. This composite landslide scar was generated by one or more collapse that occurred between 34–26 and 2 ka (Linde et al. 2014), producing rock/debris avalanches (Romagnoli et al. 2009). The moderate susceptibility in the Rina Grande–Le Schicciole depression is mainly related to the presence of destabilizing factors, mainly slope and the presence of Breccia and Pyroclastic deposit units (Apuani et al. 2005b). Finally, the NE sector of the island shows low susceptibility to intrusion-related landslides and allows estimating unlikely the development of landslides in the case of intrusion in this area.

Conclusions

Intrusion-related landslide susceptibility at the Island of Stromboli has been evaluated coupling (1) landslide susceptibility evaluation by random forest (RF) technique and (2) the probabilistic volcanic vent opening distribution, as proxy for magma injection, using QVAST tool.

The results can be summarized as follows:

- 179 areas affected by mass-wasting phenomena were identified, mainly located within the SdF and "Rina Grande-Le Schicciole" depressions. Sea-cliffs are affected by rock-falls, related to strong coastal regression;

- areas affected by high to very high landslide susceptibility include the SdF, the upper part of the volcanic edifice and the coastal cliffs;
- landslide destabilizing factors are the slope, the aspect, the terrain roughness, land cover and litho-technical features of the outcropping rocks;
- the highest probability of a fresh vent opening is the area that is closest to the eruptive vent of the SdF depression. Moreover, the VSM highlights a probabilistic vent opening distribution elongated towards NE, highlighting the presence of a probability of new vent opening where previous activity in the Holocene ensures the possibility of future eruptive vents;
- areas with higher probability of intrusion-related landslides are located in the upper part of the SdF, the same area characterized by the occurrence of mass-wasting during the 1985, 2002–2003, 2007 and 2014 flank eruptions.

These results have the added value of producing a model that can be adapted, modified, updated and generalized in other geological contexts and in particular to other (mainly mafic to intermediate) volcanoes affected by intrusion-related slope instability. In addition to that, the conceptual models resulting from this work have direct implications for the monitoring and the hazard assessment at Stromboli volcano.

References

Abruzzese D (1935) Attività dello Stromboli dal 1930 al 1934. Boll Sism It 33:118–121

Abruzzese D (1937) Attività dello Stromboli dal 1934 al 1936. Bull Volcanol 11:205–210

Abruzzese D (1940) Attività dello Stromboli dal 1937 al giugno 1939. Bull Volcanol 7:57–66

Anderson EM (1937) IX.—the dynamics of the formation of cone-sheets, ring-dykes, and caldron-subsidences. P Roy Soc Edinb 56:128–157

Arrighi S, Rosi M, Tanguy JC, Courtillot V (2004) Recent eruptive history of Stromboli (Aeolian Islands, Italy) determined from high-accuracy archeomagnetic dating. J Geophys Res 31(19):L19603

Apuani T, Corazzato C, Cancelli A, Tibaldi A (2005a) Stability of a collapsing volcano (Stromboli, Italy): limit equilibrium analysis and numerical modelling. J Volcanol Geotherm Res 144(1):191–210

Apuani T, Corazzato C, Cancelli A, Tibaldi A (2005b) Physical and mechanical properties of rock masses at Stromboli: a dataset for volcano instability evaluation. B Eng Geol Environ 64(4):419–431

Bartolini S, Cappello A, Martí J, Negro C (2013) QVAST: a new quantum GIS plugin for estimating volcanic susceptibility. Nat Hazard Earth Sys 13(11):3031–3042

Becerril L, Cappello A, Galindo I, Neri M, Del Negro C (2013) Spatial probability distribution of future volcanic eruptions at el Hierro Island (Canary Islands, Spain). J Volcanol Geotherm Res 257:21–30

Blackburn EA, Wilson L, Sparks RJ (1976) Mechanisms and dynamics of strombolian activity. J Geol Soc Lond 132(4):429–440

Bonaccorso A (1998) Evidence of a dyke-sheet intrusion at Stromboli Volcano inferred through continuous tilt. Geophys Res Lett 25(22):4225–4228

Bonaccorso A, Calvari S, Garfì G, Lodato L, Patanè D (2003) Dynamics of the December 2002 flank failure and tsunami at Stromboli Volcano inferred by volcanological and geophysical observations. J Geophys Res 30(18):1941

Breiman L (2001) Random forests. Mach Learn 45:5–32

Calvari S, Spampinato L, Lodato L, Harris AJL, Patrick MR, Dehn J, Burton MR, Andronico D (2005) Chronology and complex volcanic processes during the 2002–2003 flank eruption at Stromboli Volcano (Italy) reconstructed from direct observations and surveys with a handheld thermal camera. J Geophys Res 110:B02201

Calvari S, Lodato L, Steffke A, Cristaldi A, Harris AJL, Spampinato L, Boschi E (2010) The 2007 Stromboli eruption: event chronology and effusion rates using thermal infrared data. J Geophys Res 115:B04201

Calvari S, Branca S, Corsaro R, De Beni E, Miraglia L, Norini G, Wijbrans J, Boschi E (2011) Reconstruction of the eruptive activity on the NE sector of Stromboli Volcano: timing of flank eruptions since 15 ka. Bull Volcanol 73(1):101–112

Calvari S, Bonaccorso A, Madonia P, Neri M, Liuzzo M, Salerno GG, Behncke B, Caltabiano T, Cristaldi A, Giuffrida G, La Spina A, Marotta E, Ricci T, Spampinato L (2014) Major eruptive style changes induced by structural modifications of a shallow conduit system: the 2007–2012 Stromboli case. B Volcanol 76(7):1–15

Calvari S, Intrieri E, Di Traglia F, Bonaccorso A, Casagli N, Cristaldi A (2016) Monitoring crater-wall collapse at active volcanoes: a study of the 12 January 2013 event at Stromboli. B Volcanol 78(5):1–16

Capaldi G, Guerra I, Lo Bascio A, Luongo G, Pece R, Rapolla A, Scarpa R, Del Pezzo E, Martini M, Ghiara MR, Lirer L, Munno R, La Volpe L (1978) Stromboli and its 1975 eruption. Bull Volcanol 41:1–27

Cappello A, Neri M, Acocella V, Gallo G, Vicari A, Del Negro C (2012) Spatial vent opening probability map of Etna volcano (Sicily, Italy). Bull Volcanol 74(9):2083–2094

Carlà T, Intrieri E, Di Traglia F, Nolesini T, Gigli G, Casagli N (2016) Guidelines on the use of inverse velocity method as a tool for setting alarm thresholds and forecasting landslides and structure collapses. Landslides 1–18. doi: 10.1007/s10346-016-0731-5

Casalbore D, Romagnoli C, Chiocci F, Frezza V (2010) Morpho-sedimentary characteristics of the volcaniclastic apron around Stromboli volcano (Italy). Mar Geol 269(3):132–148

Catani F, Lagomarsino D, Segoni S, Tofani V (2013) Landslide susceptibility estimation by random forests technique: sensitivity and scaling issues. Nat Hazards Earth Syst 13(11):2815–2831

Ciampalini A, Raspini F, Bianchini S, Frodella W, Bardi F, Lagomarsino D, Di Traglia F, Moretti S, Proietti C, Pagliara P, Onori R, Corazza A, Duro A, Basile G, Casagli N (2015) Remote sensing as tool for development of landslide databases: the case of the Messina Province (Italy) geodatabase. Geomorphology 249:103–118

Corazzato C, Francalanci L, Menna M, Petrone CM, Renzulli A, Tibaldi A, Vezzoli L (2008) What controls sheet intrusion in volcanoes? Structure and petrology of the Stromboli sheet complex, Italy. J Volcanol Geotherm Res 173(1):26–54

De Fino M, La Volpe L, Falsaperla S, Frazzetta G, Neri G, Francalanci L, Rosi M, Sbrana A (1988) The Stromboli eruption of December 6, 1985–April 25, 1986: volcanological, petrological and seismological data. Rend Soc Ital Mineral Petrol 43:1021–1038

Di Traglia F, Nolesini T, Intrieri E, Mugnai F, Leva D, Rosi M, Casagli N (2014a) Review of ten years of volcano deformations recorded by the ground-based InSAR monitoring system at Stromboli Volcano: a tool to mitigate volcano flank dynamics and intense volcanic activity. Earth-Sci Rev 139:317–335

Di Traglia F, Intrieri E, Nolesini T, Bardi F, Del Ventisette C, Ferrigno F, Frangioni S, Frodella W, Gigli G, Lotti A, Stefanelli CT, Tanteri L, Leva D, Casagli N (2014b) The ground-based InSAR monitoring system at Stromboli Volcano: linking changes in displacement rate and intensity of persistent volcanic activity. Bull Volcanol 76:786

Di Traglia F, Battaglia M, Nolesini T, Lagomarsino D, Casagli N (2015) Shifts in the eruptive style at Stromboli in 2010-2014 revealed by ground-based InSAR data. Sci Rep 5. doi: 10.1038/srep13569

Falsaperla S, Lanzafame G, Longo V, Spampinato S (1999) Regional stress field in the area of Stromboli (Italy): insights into structural data and crustal tectonic earthquakes. J Volcanol Geotherm Res 88(3):147–166

Felpeto A, Martí J, Ortiz R (2007) Automatic GIS-based system for volcanic hazard assessment. J Volcanol Geotherm Res 166(2):106–116

Finizola A, Sortino F, Lénat JF, Valenza M (2002) Fluid circulation at Stromboli Volcano (Aeolian Islands, Italy) from self-potential and CO 2 surveys. J Volcanol Geotherm Res 116(1):1–18

Finizola A, Sortino F, Lénat JF, Aubert M, Ripepe M, Valenza M (2003) The summit hydrothermal system of Stromboli. New insights from self-potential, temperature, CO2 and fumarolic fluid measurements, with structural and monitoring implications. Bull Volcanol 65(7):486–504

Gasparini P, Lirer L, Luongo G (1968) Caratteristiche petrochimiche e fisiche della lava emessa dallo Stromboli nell'aprile del 1967. Ann Osserv Vesuv 8:13–18

Hazlett RW, Buesch D, Anderson JL, Elan R, Scandone R (1991) Geology failure conditions and implications of seismogenic avalanches of the 1944 eruption at Vesuvius, Italy. J Volcanol Geotherm Res 47:249–264

Kokelaar P, Romagnoli C (1995) Sector collapse, sedimentation and clast population evolution at an active island-arc volcano: Stromboli, Italy. B Volcanol 57(4):240–262

Le Corvec N, Menand T, Lindsay J (2013) Interaction of ascending magma with pre-existing crustal fractures in monogenetic basaltic volcanism: an experimental approach. J Geophys Res-Sol Ea 118(3):968–984

Linde N, Baron L, Ricci T, Finizola A, Revil A, Muccini F, Cocchi L, Carmisciano C (2014) 3-D density structure and geological evolution of Stromboli Volcano(Aeolian Islands, Italy) inferred from land-based and sea-surface gravity data. J Volcanol Geotherm Res 273:58–69

Major JJ, Pierson TC, Dinehart RL, Costa JE (2000) Sediment yield following severe volcanic disturbance—a two-decade perspective from mount St. Helens Geology 28(9):819–822

Marsella M, Baldi P, Coltelli M, Fabris M (2012) The morphological evolution of the Sciara del Fuoco since 1868: reconstructing the effusive activity at Stromboli Volcano. Bull Volcanol 74:231–248

Marti J, Felpeto A (2010) Methodology for the computation of volcanic susceptibility: an example for mafic and felsic eruptions on Tenerife (Canary Islands). J Volcanol Geotherm Res 195:69–77

Nave R, Isaia R, Vilardo G, Barclay J (2010) Re-assessing volcanic hazard maps for improving volcanic risk communication: application to Stromboli Island, Italy. J Maps 2010:260–269

Neri M, Lanzafame G, Acocella V (2008) Dike emplacement and related hazard in volcanoes with sector collapse: the 2007 Stromboli eruption. J Geol Soc Lond 165:883–886

Neri M, Lanzafame G (2009) Structural features of the 2007 Stromboli eruption. J Volcanol Geotherm Res 182:137–144

Nolesini T, Di Traglia F, Del Ventisette C, Moretti S, Casagli N (2013) Deformations and slope instability on Stromboli Volcano: integration of GBInSAR data and analogue modeling. Geomorphology 180–181:242–254

Rittmann A (1931) Der Ausbruch des Stromboli am 11 September 1930. Zeits f Vulkanol 14:47–77

Rizzo AL, Federico C, Inguaggiato S, Sollami A, Tantillo M, Vita F, Bellomo S, Longo M, Grassa F, Liuzzo M (2015) The 2014 effusive eruption at Stromboli Volcano (Italy): inferences from soil CO2 flux and 3He/4He ratio in thermal waters. Geophys Res Lett 42(7):2235–2243

Romagnoli C, Casalbore D, Chiocci FL, Bosman A (2009) Offshore evidence of large-scale lateral collapse on the eastern flank of Stromboli, Italy, due to structurally-controlled, bi-lateral flank instability. Mar Geol 262(1):1–13

Rosi M, Pistolesi M, Bertagnini A, Landi P, Pompilio M, Di Roberto A (2013) Stromboli Volcano, Aeolian Islands (Italy): present eruptive activity and hazard. In: Lucchi F, Peccerillo a, Keller J, Tranne CA, Rossi PL (eds) Geology of the Aeolian Islands (Italy). Geol Soc Lond Mem 37(1):473–490

Rubin AM (1995) Propagation of magma-filled cracks. Annu Rev Earth Pl Sc 23:287–336

Salvatici T, Di Roberto A, Di Traglia F, Bisson M, Morelli S, Fidolini F, Bertagnini A, Pompilio M, Hungr O, Casagli N (2016) From hot rocks to glowing avalanches: numerical modelling of gravity-induced pyroclastic density currents and hazard maps at the Stromboli Volcano (Italy). Geomorphology 273:93–106

Schaefer LN, Kendrick JE, Oommen T, Lavallée Y, Chigna G (2015) Geomechanical rock properties of a basaltic volcano. Front Earth Sci 3:29

Siebert L (1984) Large volcanic debris avalanches: characteristics of source areas, deposits, and associated eruptions. J Volcanol Geotherm Res 22(3–4):163–197

Sosio R, Crosta GB, Hungr O (2012) Numerical modeling of debris avalanche propagation from collapse of volcanic edifices. Landslides 9(3):315–334

Takada A (1994) The influence of regional stress and magmatic input on styles of monogenetic and polygenetic volcanism. J Geophys Res-Sol Ea 99(B7):13563–13573

Tarquini S, Isola I, Favalli M, Mazzarini F, Bisson M, Pareschi MT, Boschi E (2007) TINITALY/01: a new triangular irregular network of Italy. Ann Geophys 50(3):407–425

Tarquini S, Vinci S, Favalli M, Doumaz F, Fornaciai A, Nannipieri L (2012) Release of a 10-m-resolution DEM for the Italian territory: comparison with global-coverage DEMs and anaglyph-mode exploration via the web. Comput Geosci 38:168–170

Tibaldi A (2001) Multiple sector collapse at Stromboli Volcano, Italy: how they work. Bull Volcanol 63:112–125

Tibaldi A, Corazzato C, Gamberi F, Marani M (2009) Subaerial-submarine evidence of structures feeding magma to Stromboli Volcano, Italy, and relations with edifice flank failure and creep. Tectonophysics 469:112–136

Tibaldi A (2010) A new geological map of Stromboli Volcano (Tyrrhenian sea, Italy) based on application of lithostratigraphic and UBS units. Geol Soc Am Spec Publ 464:33–49

Tinti S, Manucci A, Pagnoni G, Armigliato A, Zaniboni F (2005) The 30th December 2002 tsunami in Stromboli: sequence of the events reconstructed from the eyewitness accounts. Nat Hazards Earth Syst Sci 5:763–775

Voight B, Elsworth D (1997) Failure of volcano slopes. Geotechnique 47:131

Voight B, Komorowski J-C, Norton G, Belousov A, Belousova M, Boudon G, Francis P, Franz W, Sparks S, Young S (2002) The 1997 boxing day sector collapse and debris avalanche, Soufrière Hills volcano, Montserrat, B.W.I. In: Druitt T, Kokelaar BP (eds) The eruption of Soufrière Hills volcano, Montserrat, from 1995–1999. Mem Geol Soc Lond 21:363–407

Zakšek K, Hort M, Lorenz E (2015) Satellite and ground based thermal observation of the 2014 effusive eruption at Stromboli Volcano. Remote Sens 7(12):17190–17211

F. Di Traglia (✉) · **E. Artesi** · **T. Nolesini** · **A. Ciampalini** · **D. Lagomarsino** · **N. Casagli**
Dipartimento di Scienze della Terra,
Università degli Studi di Firenze,
Via La Pira 4, 50121, Florence, Italy
e-mail: federico.ditraglia@unifi.it

S. Bartolini · **J. Martí**
Group of Volcanology, (SIMGEO-UB) CSIC,
Institute of Earth Sciences Jaume Almera,
c/Lluis Sole Sabaris s/n, 08028, Barcelona, Spain